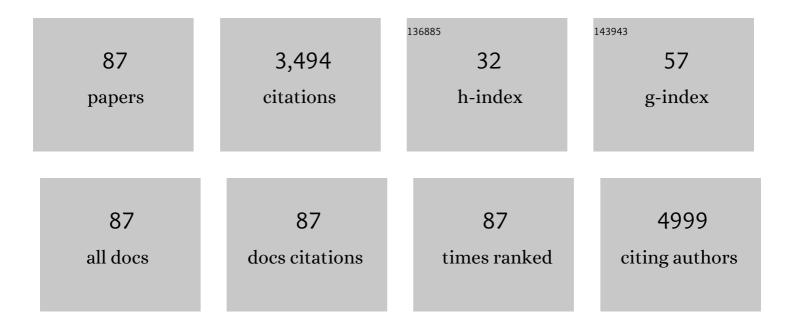
List of Publications by Year in descending order

Source: https://exaly.com/author-pdf/8814037/publications.pdf Version: 2024-02-01



LUMEI TIAN

#	Article	IF	CITATIONS
1	Highâ€Energy/Power and Lowâ€Temperature Cathode for Sodiumâ€Ion Batteries: In Situ XRD Study and Superior Fullâ€Cell Performance. Advanced Materials, 2017, 29, 1701968.	11.1	350
2	A Scalable Strategy To Develop Advanced Anode for Sodium-Ion Batteries: Commercial Fe <sub>3</sub> O <sub>4</sub> -Derived Fe <sub>3</sub> O <sub>4</sub> @FeS with Superior Full-Cell Performance. ACS Applied Materials & Interfaces, 2018, 10, 3581-3589.	4.0	209
3	In Situ Binding Sb Nanospheres on Graphene via Oxygen Bonds as Superior Anode for Ultrafast Sodium-Ion Batteries. ACS Applied Materials & Interfaces, 2016, 8, 7790-7799.	4.0	167
4	A Practicable Li/Naâ€lon Hybrid Full Battery Assembled by a Highâ€Voltage Cathode and Commercial Graphite Anode: Superior Energy Storage Performance and Working Mechanism. Advanced Energy Materials, 2018, 8, 1702504.	10.2	142
5	Nanoeffects promote the electrochemical properties of organic Na2C8H4O4 as anode material for sodium-ion batteries. Nano Energy, 2015, 13, 450-457.	8.2	139
6	Pseudocapacitance-boosted ultrafast Na storage in a pie-like FeS@C nanohybrid as an advanced anode material for sodium-ion full batteries. Nanoscale, 2018, 10, 9218-9225.	2.8	135
7	Highâ€Performance and Lowâ€Temperature Lithium–Sulfur Batteries: Synergism of Thermodynamic and Kinetic Regulation. Advanced Energy Materials, 2018, 8, 1703638.	10.2	124
8	Metastable Marcasite-FeS <sub>2</sub> as a New Anode Material for Lithium Ion Batteries: CNFs-Improved Lithiation/Delithiation Reversibility and Li-Storage Properties. ACS Applied Materials & Interfaces, 2017, 9, 10708-10716.	4.0	122
9	Host Materials Transformable in Tumor Microenvironment for Homing Theranostics. Advanced Materials, 2017, 29, 1605869.	11.1	121
10	Shale-like Co <sub>3</sub> O <sub>4</sub> for high performance lithium/sodium ion batteries. Journal of Materials Chemistry A, 2016, 4, 8242-8248.	5.2	108
11	Dual-carbon enhanced silicon-based composite as superior anode material for lithium ion batteries. Journal of Power Sources, 2016, 307, 738-745.	4.0	81
12	Supramolecular Nano-Aggregates Based on Bis(Pyrene) Derivatives for Lysosome-Targeted Cell Imaging. Journal of Physical Chemistry C, 2013, 117, 26811-26820.	1.5	79
13	A promising PMHS/PEO blend polymer electrolyte for all-solid-state lithium ion batteries. Dalton Transactions, 2018, 47, 14932-14937.	1.6	67
14	Target construction of ultrathin graphitic carbon encapsulated FeS hierarchical microspheres featuring superior low-temperature lithium/sodium storage properties. Journal of Materials Chemistry A, 2018, 6, 7997-8005.	5.2	62
15	Co <sub>3</sub> O <sub>4</sub> Nanospheres Embedded in a Nitrogen-Doped Carbon Framework: An Electrode with Fast Surface-Controlled Redox Kinetics for Lithium Storage. ACS Energy Letters, 2017, 2, 52-59.	8.8	61
16	Radical Mechanism of Isocyanide-Alkyne Cycloaddition by Multicatalysis of Ag2CO3, Solvent, and Substrate. ACS Catalysis, 2015, 5, 6177-6184.	5.5	54
17	Three-dimensional carbon nanotube networks enhanced sodium trimesic: a new anode material for sodium ion batteries and Na-storage mechanism revealed by ex situ studies. Journal of Materials Chemistry A, 2017, 5, 16622-16629.	5.2	54
18	An FeP@C nanoarray vertically grown on graphene nanosheets: an ultrastable Li-ion battery anode with pseudocapacitance-boosted electrochemical kinetics. Nanoscale, 2019, 11, 1304-1312.	2.8	53

#	Article	IF	CITATIONS
19	Bis-pyrene-based supramolecular aggregates with reversibly mechanochromic and vapochromic responsiveness. Journal of Materials Chemistry C, 2014, 2, 1887.	2.7	52
20	A new strategy for developing superior electrode materials for advanced batteries: using a positive cycling trend to compensate the negative one to achieve ultralong cycling stability. Nanoscale Horizons, 2016, 1, 496-501.	4.1	51
21	Multiple heterointerfaces boosted de-/sodiation kinetics towards superior Na storage and Na-Ion full battery. Journal of Materials Chemistry A, 2018, 6, 6578-6586.	5.2	50
22	Synergistic mediation of sulfur conversion in lithium–sulfur batteries by a Gerber tree-like interlayer with multiple components. Journal of Materials Chemistry A, 2017, 5, 11255-11262.	5.2	49
23	2D few-layer iron phosphosulfide: a self-buffer heterophase structure induced by irreversible breakage of P–S bonds for high-performance lithium/sodium storage. Journal of Materials Chemistry A, 2019, 7, 1529-1538.	5.2	48
24	Three novel 1D lanthanide-carboxylate polymeric complexes: syntheses, crystal structures and magnetic analyses. Dalton Transactions, 2013, 42, 8504.	1.6	41
25	Full Protection for Graphene-Incorporated Micro-/Nanocomposites Containing Ultra-small Active Nanoparticles: the Best Li-Storage Properties. Particle and Particle Systems Characterization, 2015, 32, 1020-1027.	1.2	41
26	Do the bridging oxygen bonds between active Sn nanodots and graphene improve the Li-storage properties?. Energy Storage Materials, 2016, 5, 214-222.	9.5	41
27	The in-situ-prepared micro/nanocomposite composed of Sb and reduced graphene oxide as superior anode for sodium-ion batteries. Journal of Alloys and Compounds, 2016, 672, 72-78.	2.8	39
28	An Efficient Strategy for Self-Assembly of DNA-Mimic Homochiral 1D Helical Cu(II) Chain from Achiral Flexible Ligand by Spontaneous Resolution. Inorganic Chemistry, 2016, 55, 3378-3383.	1.9	37
29	Understanding the electrochemical properties of A <sub>2</sub> MSiO <sub>4</sub> (A = Li and Na; M =) Tj E calculations. Journal of Materials Chemistry A, 2016, 4, 17455-17463.	ETQq1 1 0.78 5.2	4314 rgBT (0 35
30	Tailoring Coral-Like Fe <sub>7</sub> Se <sub>8</sub> @C for Superior Low-Temperature Li/Na-Ion Half/Full Batteries: Synthesis, Structure, and DFT Studies. ACS Applied Materials & Interfaces, 2019, 11, 47886-47893.	4.0	35
31	Pseudocapacitive sodium storage of Fe1â^'xS@N-doped carbon for low-temperature operation. Science China Materials, 2020, 63, 505-515.	3.5	35
32	A New Multifunctional Zinc–Organic Framework with Rare Interpenetrated Tripillared Bilayers as a Luminescent Probe for Detecting Ni <sup>2+</sup> and PO <sub>4</sub> <sup>3–</sup> in Water. Crystal Growth and Design, 2020, 20, 5120-5128.	1.4	35
33	Recent advances of transformable nanoparticles for theranostics. Chinese Chemical Letters, 2017, 28, 1808-1816.	4.8	34
34	LiV <sub>3</sub> O <sub>8</sub> nanorods as cathode materials for high-power and long-life rechargeable lithium-ion batteries. RSC Advances, 2014, 4, 25494-25501.	1.7	33
35	Three-dimensional hierarchical Ni <sub>3</sub> Se <sub>2</sub> nanorod array as binder/carbon-free electrode for high-areal-capacity Na storage. Nanoscale, 2018, 10, 18942-18948.	2.8	30
36	Synergistic Design of Cathode Region for the High-Energy-Density Li–S Batteries. ACS Applied Materials & Interfaces, 2016, 8, 28689-28699.	4.0	29

#	Article	IF	CITATIONS
37	Diverse Structures Based on a Heptanuclear Cobalt Cluster with 0D to 3D Metal–Organic Frameworks: Magnetism and Application in Batteries. Chemistry - A European Journal, 2018, 24, 1962-1970.	1.7	29
38	Rational design of phenoxazine-based donor–acceptor–donor thermally activated delayed fluorescent molecules with high performance. Physical Chemistry Chemical Physics, 2015, 17, 20014-20020.	1.3	28
39	Mechanistic understanding of domino cyclization between gem-dialkylthio vinylallenes and benzylamine towards economic synthesis: a computational study. Green Chemistry, 2014, 16, 2653.	4.6	27
40	Porous Amorphous Co <sub>2</sub> P/N,Bâ€Coâ€doped Carbon Composite as an Improved Anode Material for Sodiumâ€ion Batteries. ChemElectroChem, 2017, 4, 1395-1401.	1.7	27
41	Decametallic Co <sup>II</sup> â€Clusterâ€Based Microporous Magnetic Framework with a Semirigid Multicoordinating Ligand. Chemistry - A European Journal, 2013, 19, 5097-5103.	1.7	26
42	Computational study on optical and electronic properties of the "CHâ€IN substituted emitting materials based on spirosilabifluorene derivatives. Computational and Theoretical Chemistry, 2008, 862, 85-91.	1.5	25
43	2D Fe <sub>2</sub> O <sub>3</sub> nanosheets with bi-continuous pores inherited from Fe-MOF precursors: an advanced anode material for Li-ion half/full batteries. 2D Materials, 2019, 6, 045022.	2.0	23
44	Turn-on fluorescence in a stable Cd(II) metal-organic framework for highly sensitive detection of Cr3+ in water. Dyes and Pigments, 2020, 178, 108359.	2.0	23
45	Flexible paper electrodes constructed from Zn <sub>2</sub> GeO <sub>4</sub> nanofibers anchored with amorphous carbon for advanced lithium ion batteries. Journal of Materials Chemistry A, 2016, 4, 2055-2059.	5.2	21
46	Divergent Reactions between αâ€Imino Rhodium Carbenoids and 1,3â€Diketones: Substrateâ€Controlled O–H versus C–H Insertion. European Journal of Organic Chemistry, 2017, 2017, 1289-1293.	1.2	20
47	Fabrication of functionalized polysulfide reservoirs from large graphene sheets to improve the electrochemical performance of lithium–sulfur batteries. Physical Chemistry Chemical Physics, 2015, 17, 23481-23488.	1.3	19
48	Target encapsulating NiMoO4 nanocrystals into 1D carbon nanofibers as free-standing anode material for lithium-ion batteries with enhanced cycle performance. Journal of Alloys and Compounds, 2020, 830, 154648.	2.8	19
49	Tuning the color of thermally activated delayed fluorescent properties for spiro-acridine derivatives by structural modification of the acceptor fragment: a DFT study. RSC Advances, 2015, 5, 18588-18592.	1.7	18
50	Alkaliâ€Metalâ€Ionâ€Functionalized Graphene Oxide as a Superior Anode Material for Sodiumâ€Ion Batteries. Chemistry - A European Journal, 2016, 22, 8152-8157.	1.7	18
51	Dualâ€Carbon Enhanced FeP Nanorods Vertically Grown on Carbon Nanotubes with Pseudocapacitanceâ€Boosted Electrochemical Kinetics for Superior Lithium Storage. Advanced Electronic Materials, 2019, 5, 1900006.	2.6	16
52	Mechanism Study of the Intramolecular Anti-Michael Addition of <i>N</i> -Alkylfurylacrylacetamides. Journal of Organic Chemistry, 2012, 77, 8744-8749.	1.7	15
53	Construction of electrical "highway―to significantly enhance the redox kinetics of normal hierarchical structured materials of MnO. Journal of Materials Chemistry A, 2018, 6, 1663-1670.	5.2	15
54	[DBUâ€H] <sup>+</sup> and H <sub>2</sub> 0 as effective catalyst form for 2,3â€dihydropyrido[2,3â€ <i>d</i> ]pyrimidinâ€4(1 <i>H</i> )â€ones: A DFT Study. Journal of Computational Chemistry, 2015, 36, 1295-1303.	1.5	14

#	Article	IF	CITATIONS
55	An <i>in situ</i> â€Fabricated Composite Polymer Electrolyte Containing Largeâ€Anion Lithium Salt for Allâ€Solidâ€State LiFePO <sub>4</sub> /Li Batteries. ChemElectroChem, 2017, 4, 2293-2299.	1.7	14
56	Selective chiral symmetry breaking and luminescence sensing of a Zn( <scp>ii</scp> ) metal–organic framework. Dalton Transactions, 2018, 47, 7934-7940.	1.6	14
57	In situ construction of ligand nano-network to integrin $\hat{I}\pm v\hat{I}^23$ for angiogenesis inhibition. Chinese Chemical Letters, 2020, 31, 3107-3112.	4.8	14
58	Charge control of the formation of two neutral/cationic metal–organic frameworks based on neutral/cationic triangular clusters and isonicotinic acid: structure, gas adsorption and magnetism. CrystEngComm, 2018, 20, 5402-5408.	1.3	13
59	Theoretical investigations of the realization of sky-blue to blue TADF materials <i>via</i> CH/N and H/CN substitution at the diphenylsulphone acceptor. Journal of Materials Chemistry C, 2019, 7, 6685-6691.	2.7	13
60	Theoretical design of blue emitting materials based on symmetric and asymmetric spirosilabifluorene derivatives. Theoretical Chemistry Accounts, 2008, 119, 489-500.	0.5	12
61	Micro/Nanoengineered αâ€Fe 2 O 3 Nanoaggregate Conformably Enclosed by Ultrathin Nâ€Doped Carbon Shell for Ultrastable Lithium Storage and Insight into Phase Evolution Mechanism. Chemistry - A European Journal, 2020, 26, 853-862.	1.7	12
62	Two Metal–Organic Frameworks Based on Hexanuclear Cobalt–Hydroxyl Clusters or a Manganese–Hydroxyl Chain from Triangular [MII3(μ3-OH)] (M = Co and Mn) Units: Antiferromagnetic and Spin-Canting Antiferromagnetic Ordering with Soft-Magnetic Behavior. Inorganic Chemistry, 2020, 59, 12017-12024.	1.9	12
63	Transition metal phosphite complexes: from one-dimensional chain, two-dimensional sheet, to three-dimensional architecture with unusual magnetic properties. CrystEngComm, 2014, 16, 1071-1078.	1.3	11
64	A stable luminescent zinc–organic framework as a dual-sensor toward Cu <sup>2+</sup> and Cr <sub>2</sub> O <sub>7</sub> <sup>2â^'</sup> , and excellent platform-encapsulated Ln <sup>3+</sup> for systematic color tuning and white-light emission. New Journal of Chemistry, 2019, 43, 13794-13801.	1.4	11
65	Silver-mediated radical coupling reaction of isocyanides and alcohols/phenols in the presence of water: unprecedented hydration and radical coupling reaction sequence. Organic and Biomolecular Chemistry, 2017, 15, 1580-1583.	1.5	10
66	Tuning the electronic and optical properties of diphenylsulphone based thermally activated delayed fluorescent materials via structural modification: A theoretical study. Dyes and Pigments, 2017, 143, 42-47.	2.0	10
67	Insight into electrochemical and elastic properties in AFe1-M SO4F (A = Li, Na; M = Co, Ni, Mg) cathode materials: A first principle study. Electrochimica Acta, 2017, 251, 316-323.	2.6	10
68	Tetranuclear cobalt( <scp>ii</scp> )–isonicotinic acid frameworks: selective CO <sub>2</sub> capture, magnetic properties, and derived "Co <sub>3</sub> O <sub>4</sub> ―exhibiting high performance in lithium ion batteries. Dalton Transactions, 2019, 48, 296-303.	1.6	10
69	Computational design of benzo [1,2-b:4,5-bâ€2] dithiophene based thermally activated delayed fluorescent materials. Dyes and Pigments, 2016, 127, 189-196.	2.0	9
70	A computational mechanistic study of substrate-controlled competitive O–H and C–H insertion reactions catalyzed by dirhodium( <scp>ii</scp> ) carbenoids: insight into the origin of chemoselectivity. Organic Chemistry Frontiers, 2018, 5, 2353-2363.	2.3	9
71	Assembly of metal–organic frameworks based on 4-connected 3,3′,5,5′-azobenzenetetracarboxylic acid: structures, magnetic properties, and sensing of Fe <sup>3+</sup> ions. New Journal of Chemistry, 2019, 43, 4226-4234.	1.4	8
72	Pseudocapacitive Lithium Storage of Cauliflowerâ€Like CoFe <sub>2</sub> O <sub>4</sub> for Lowâ€Temperature Battery Operation. Chemistry - A European Journal, 2020, 26, 13652-13658.	1.7	8

#	Article	IF	CITATIONS
73	Mechanistic insights on DBU catalyzed <i>î²</i> â€amination of nbs to chalcone driving by water: Multiple roles of water. Journal of Computational Chemistry, 2017, 38, 438-445.	1.5	7
74	The control effects of different scaffolds in chiral phosphoric acids: a case study of enantioselective asymmetric arylation. Catalysis Science and Technology, 2019, 9, 6482-6491.	2.1	7
75	Understanding the electrochemical properties of bulk phase and surface structures of Na <sub>3</sub> T <sup>M</sup> PO <sub>4</sub> CO <sub>3</sub> (T <sup>M</sup> = Fe, Mn, Co, Ni) from first principles calculations. Physical Chemistry Chemical Physics, 2020, 22, 25325-25334.	1.3	7
76	Li <sub>2</sub> FePO <sub>4</sub> F and its metal-doping for Li-ion batteries: an ab initio study. RSC Advances, 2014, 4, 50195-50201.	1.7	6
77	The multieffects of DMF and DBU on the [5 + 1] benzannulation of nitroethane and αâ€alkenoyl keteneâ€( <i>S,S</i> )â€acetals: Hydrogen bonding and electrostatic interactions. Journal of Computational Chemistry, 2015, 36, 731-738.	1.5	6
78	Mechanistic insight on ( <i>E</i> )â€methyl 3â€(2â€aminophenyl)acrylate cyclization reaction by multicatalysis of solvent and substrate. Journal of Computational Chemistry, 2016, 37, 2386-2394.	1.5	6
79	<i>In situ</i> construction of nanonetworks from transformable nanoparticles for anti-angiogenic therapy. Journal of Materials Chemistry B, 2018, 6, 5282-5289.	2.9	5
80	2D Metalâ€Organic Framework Derived Co 3 O 4 for the Oxygen Evolution Reaction and Highâ€Performance Lithiumâ€Ion Batteries. ChemNanoMat, 2020, 6, 1770-1775.	1.5	5
81	Mechanistic investigation on N → C <sup>α</sup> → O relay via non-Brook rearrangement: reaction conditions promote synthesis of furo[3,2-c]pyridinones. Organic and Biomolecular Chemistry, 2017, 15, 9127-9138.	1.5	4
82	A mechanistic investigation into N-heterocyclic carbene (NHC) catalyzed umpolung of ketones and benzonitriles: is the cyano group better than the classical carbonyl group for the addition of NHC?. Organic Chemistry Frontiers, 2019, 6, 523-531.	2.3	4
83	Enantioselective synthesis of chiral tetrasubstituted allenes: harnessing electrostatic and noncovalent interactions in a bifunctional activation model for <i>N</i> -triflylphosphoramide catalysis. Organic Chemistry Frontiers, 2021, 8, 1510-1519.	2.3	4
84	Selective CO <sub>2</sub> adsorption and theoretical simulation of a stable Co( <scp>ii</scp> )-based metal–organic framework with tunable crystal size. CrystEngComm, 2019, 21, 1564-1569.	1.3	3
85	Mechanistic insights into Nâ€Bromosuccinimideâ€promoted synthesis of imidazo[1,2â€ <i>a</i> ]pyridine in water: Reactivity mediated by substrates and solvent. Journal of Computational Chemistry, 2018, 39, 2324-2332.	1.5	2
86	Mechanistic investigation-inspired activation mode of DBU and the function of the α-diazo group in the reaction of the α-amino ketone compound and EDA: [DBU-H] <sup>+</sup> -DMF-H <sub>2</sub> O and α-diazo as strong N-terminal nucleophiles. Organic Chemistry Frontiers, 2019, 6, 2678-2686.	2.3	2
87	How the Magnetic Field Impacts the Chiroptical Activities of Helical Copper Enantiomers. New Journal of Chemistry, 0, , .	1.4	0